EXHIBIT 2

Pathology of Acute and Chronic Coronary Stenting in Humans

Andrew Farb, MD; Giuseppe Sangiorgi, MD; Andrew J. Carter, DO; Virginia M. Walley, MD; William D. Edwards, MD; Robert S. Schwartz, MD; Renu Virmani, MD

Background—Despite the increasing use of stents, few reports have described human coronary artery morphology early and late after stenting.

Methods and Results—Histology was performed on 55 stents in 35 coronary vessels (32 native arteries and 3 vein grafts) from 32 patients. The mean duration of stent placement was 39±82 days. Fibrin, platelets, and neutrophils were associated with stent struts ≤11 days after deployment. In stents implanted for ≤3 days, only 3% of struts in contact with fibrous plaque had >20 associated inflammatory cells compared with 44% of struts embedded in a lipid core and 36% of struts in contact with damaged media ($P<0.001$). Neointimal growth determined late histological success, and increased neointimal growth correlated with increased stent size relative to the proximal reference lumen area. Neointimal thickness was greater for struts associated with medial damage than struts in contact with plaque ($P<0.0001$) or intact media ($P<0.0001$). When matched for time since treatment, neointimal cell density in stented arteries was similar to that in unstented arteries that had undergone balloon angioplasty and showed similar proteoglycan deposition.

Conclusions—Morphology after coronary stenting demonstrates early thrombus formation and acute inflammation followed by neointimal growth. Medial injury and lipid core penetration by struts result in increased inflammation. Neointima increases as the ratio of stent area to reference lumen area increases. Deployment strategies that reduce medial damage and avoid stent oversizing may lower the frequency of in-stent restenosis. (*Circulation*. 1999;99:44-52.)

Key Words: stents ■ coronary disease ■ restenosis ■ angioplasty ■ pathology

Intracoronary stent placement is being used increasingly for the treatment of atherosclerotic coronary disease. Emergency coronary artery stent placement for abrupt or threatened artery closure due to arterial dissection after PTCA has been a valuable treatment in maintaining lumen patency and reducing the need for urgent coronary bypass surgery.[1] The use of stents as primary therapy for coronary atherosclerosis has gained widespread acceptance, with reports of reduced restenosis rates in selected lesions compared with PTCA.[2,3] Currently, coronary stenting in acute myocardial infarction is under active investigation.[4]

Although stents reduce restenosis rates in carefully selected lesions,[2,3] in-stent restenosis remains a recognized clinical problem[5] and can be expected to increase in incidence as coronary stenting becomes more frequent and is used in less ideal lesions.[6] Despite the tremendous expansion of the use of coronary stents, there have been few published data on the pathology of stents deployed in human coronary arteries.[7–9] The pathology of human coronary stenting may provide insights into the biology of stent–vessel wall interaction and guide approaches to therapies to prevent or treat in-stent restenosis.

Methods

In brief, human stented coronary arteries were either embedded whole in methylmethacrylate or cut transversely for paraffin embedding (complete details of the methods will be provided by the authors on request). Histological observations consisted of plaque-stent interaction, thrombus formation, inflammation, and the presence of a neointima. In native arteries, each stent strut was evaluated with respect to contact with plaque or media, and the media was determined to be damaged or intact. The extent of arterial injury at the site of stent struts was graded by the method of Schwartz et al.[10] For arteries stented for ≤3 days, inflammation around each strut was assessed, and the following scale for inflammatory cells adjacent to struts was used: 1+, 0 to 10 inflammatory cells/strut; 2+, 11 to 20 inflammatory cells/strut; and 3+, >20 inflammatory cells/strut. Immunohistochemical staining for detection of smooth muscle cells and macrophages was performed in selected cases.

In native coronary arteries stented for >30 days, intimal thickness at each strut was measured and strut location recorded (in contact with plaque, intact media, or damaged media). A long-term histological success was defined as a percent area stenosis ≤75% and

Received May 13, 1998; revision received September 1, 1998; accepted September 16, 1998.

From the Department of Cardiovascular Pathology (A.F., A.J.C., R.V.), Armed Forces Institute of Pathology, Washington, DC; the Mayo Clinic (G.S., W.D.E., R.S.S.), Rochester, Minn; and The University of Ottawa Heart Institute and Ottawa Civic Hospital (V.M.W.), Ottawa, Ontario, Canada.

The opinions and assertions contained herein are the private views of the authors and are not to be construed as official or as reflecting the views of the Department of the Army or the Department of Defense.

Correspondence to Renu Virmani, MD, Department of Cardiovascular Pathology, Armed Forces Institute of Pathology, Washington, DC 20306-6000.

Circulation is available at http://www.circulationaha.org

TABLE 1. Distribution of Duration of Stent Implant and Type of Stent in the 142 Arterial Sections Examined

≤3 Days (14 Patients; 61 Sections)	≥4 to ≤11 Days (4 Patients; 18 Sections)	≥12 to ≤30 Days (4 Patients; 29 Sections)	>30 Days (10 Patients; 34 Sections)
41 Palmaz-Schatz	1 Palmaz-Schatz	22 Palmaz-Schatz	21 Palmaz-Schatz
13 Gianturco-Roubin	12 Gianturco-Roubin	7 Gianturco-Roubin	3 Gianturco-Roubin
4 Wiktor	5 Gianturco-Roubin II		10 Gianturco-Roubin II
3 Gianturco-Roubin II			

failure as stenosis >75%. Native coronary arteries stented for >30 days (5 stents) were compared with coronary arteries with PTCA alone (10 arteries) matched for duration of stent placement or PTCA. Staining with Alcian blue was performed to identify proteoglycans in the neointima and their component glycosaminoglycans (hyaluronic acid, chondroitin sulfate, dermatan sulfate, and heparan sulfate), and staining was repeated after 3 hours of testicular hyalidase digestion. Neointimal cell density and neointimal thickness were determined.

Results

Fifty-five stents in 35 coronary vessels (32 native coronary arteries and 3 saphenous vein bypass grafts) from 32 patients (mean age, 64±10 years; 17 men and 15 women) with stents were studied. Coronary artery stents were obtained at autopsy in 28 patients; stents in saphenous vein grafts were obtained at repeat bypass surgery in 3 patients, and a stent in a native coronary artery was obtained at the time of cardiac transplantation in 1 patient. In autopsy cases, the cause of death was acute myocardial infarction in 18 cases, sudden unexpected cardiac death in 7, and noncardiac death in 3. The mean number of stents per artery was 1.6±1.1 (range, 1 to 4 stents). The 32 native coronary stents were placed as follows: left main, n=3; left anterior descending, n=12; left circumflex, n=8; and right coronary, n=9. The indication for stenting was primary therapy in 18 and suboptimal result from PTCA or significant arterial dissection in 17. Adjunctive PTCA was

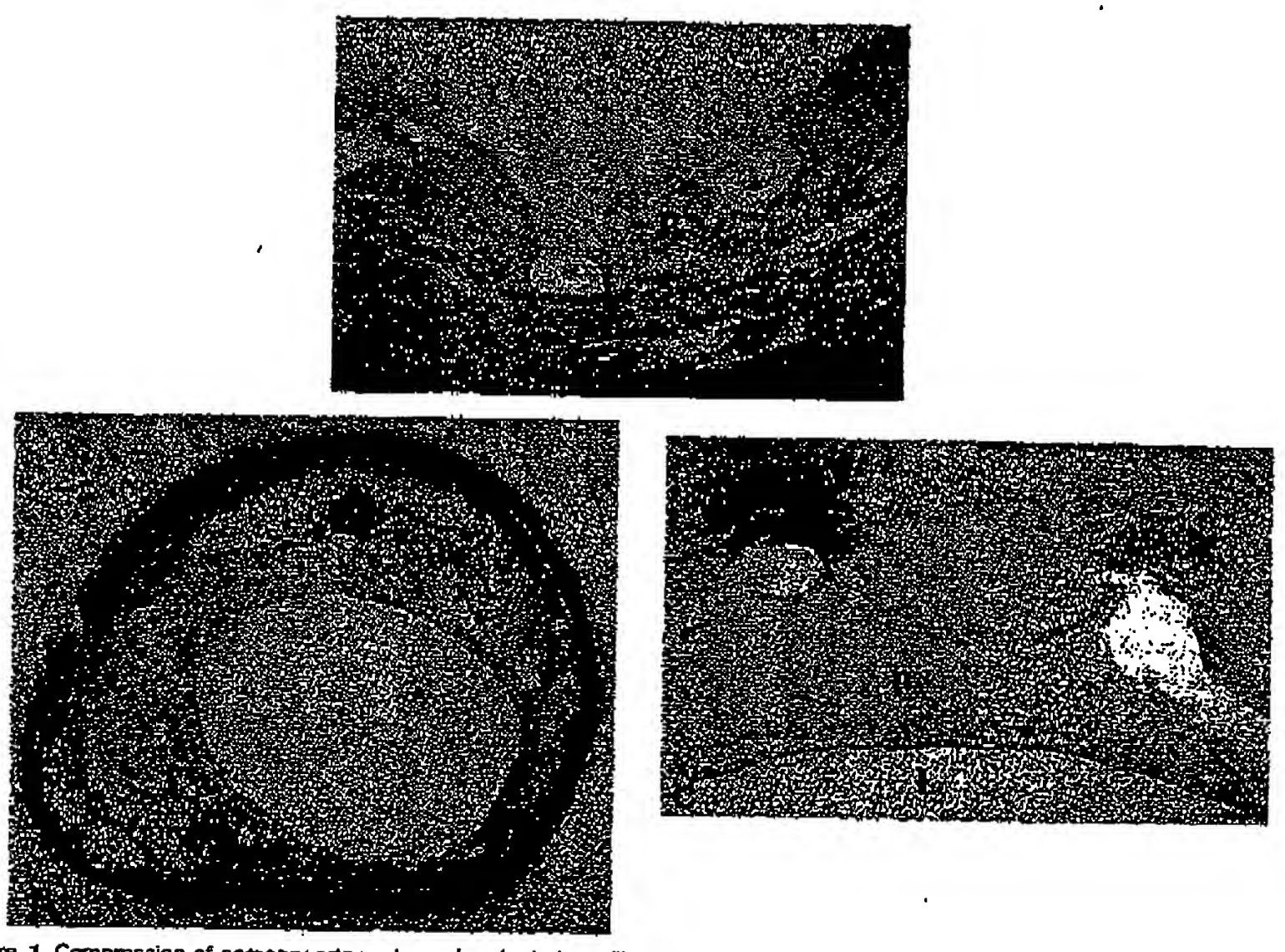

Figure 1. Compression of coronary artery plaque by stent struts (*). There is bowing of the plaque (p) into the lumen between struts of this Palmaz-Schatz stent placed 1 day antemortem (A; hematoxylin-eosin, bar=0.12 mm). Fibrous plaque compression by stent struts is present 120 days after coronary implant, seen at low (B) and high (C) powers. A layer of neointima (n) is present between struts and lumen (L). (B and C: Movat pentachrome, bars=0.12 mm.)

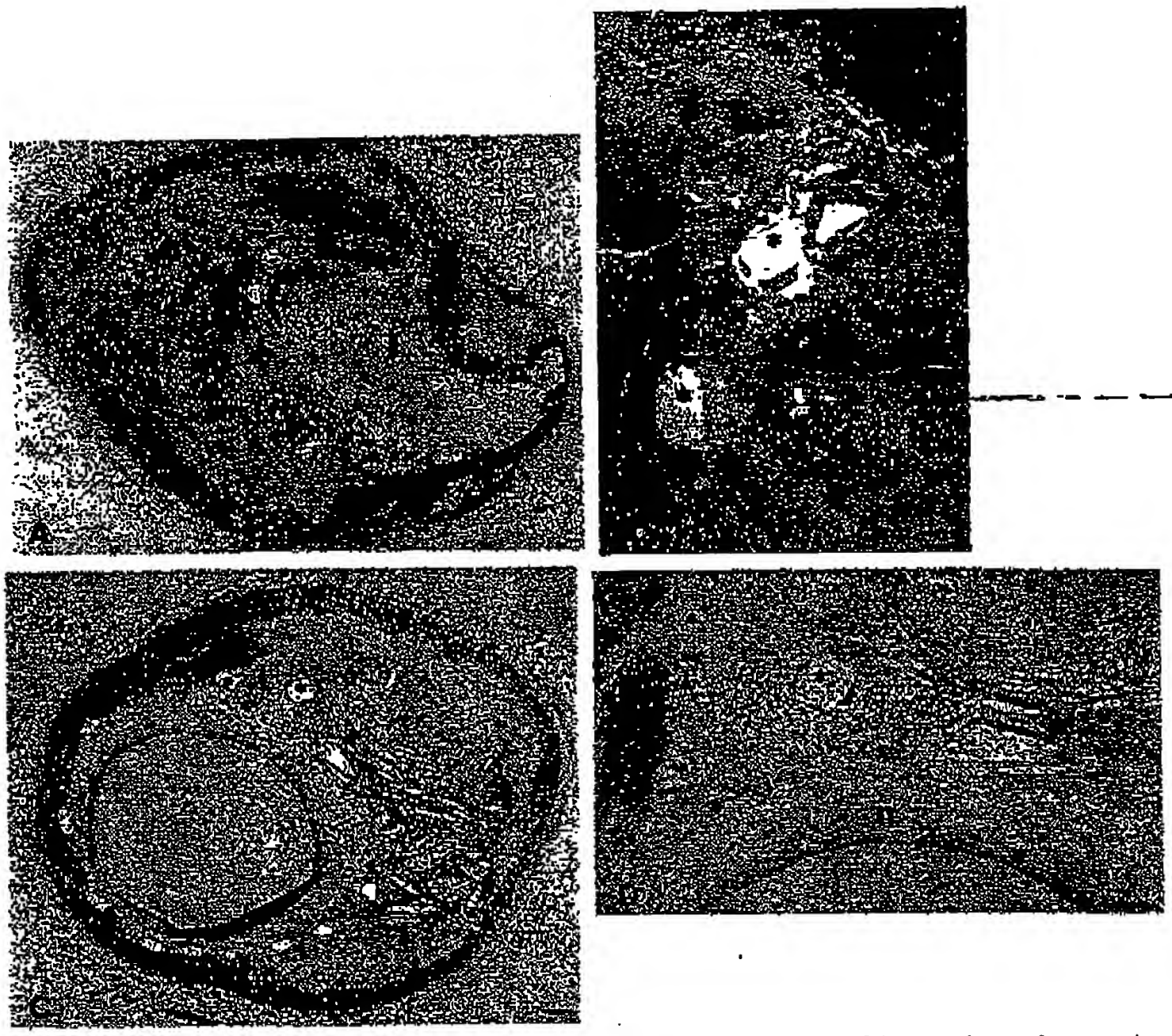

Figure 2. Focal penetration of stent struts through thin fibrous cap of fibroatheromatous plaque into necrotic core is seen at low power (A; arrowheads outline the necrotic core) and high power (B). In this case, a Palmaz-Schatz stent was placed at a site of eccentric, lipid-rich coronary plaque. Residual arterial dissection (arrow) is evident in A, resulting in focal compression of the lumen (L). Struts are identified (*) in B, and necrotic core (arrowheads) containing cholesterol clefts is seen extending toward the lumen (L). Stent struts within the necrotic core are seen at low (C) and high (D) power after Palmaz-Schatz coronary stenting 390 days antemortem. The plaque is eccentric and lipid rich. Cholesterol clefts (arrowhead) are present between struts (*), consistent with penetration of lipid core by struts at time of stent placement. Note that the neointima (n) is in close proximity to the struts and cholesterol clefts. (Movat pentachrome; A and B, bars=0.12 mm; C and D, bars=0.20 mm.)

performed in all cases, along with atherectomy in 4 cases. The clinical diagnoses at the time of stenting were unstable angina in 13 cases, acute myocardial infarction in 7, and stable angina in 12. Bailout stenting, defined as stenting for threatened or acute vessel closure after PTCA, was performed in 6 patients.

The mean duration of stent implantation for the 55 stents was 39±82 days (range, 0.5 to 390 days), with 25 stents (from 14 patients) examined ≤3 days after implantation, 8 stents (4 patients) from ≥4 to ≤11 days, 11 stents (4 patients) from ≥12 to ≤30 days, and 11 stents (10 patients) after >30 days (mean, 175±105 days). A total of 142 arterial sections (137 native coronary arteries and 5 saphenous vein bypass grafts) containing stents were analyzed (Table 1).

Plaque compression (Figure 1) by stent struts was observed in 30 (94%) of 32 patients and 129 (91%) of 142 arterial sections and was seen in all stent designs. A lipid core was present in the plaque in 66 sections (21 of 32 patients), and the core was focally penetrated by stent struts in 17 sections (26%; 11 patients; Figure 2): 14 of 44 sections containing a Palmaz-Schatz stent, 2 of 13 containing a Gianturco-Roubin stent, 0 of 1 containing a Wiktor stent, and 1 of 8 containing a Gianturco-Roubin II stent.

Platelet-rich thrombi were associated with stent struts (Figure 3A) in 65 of the 142 arterial sections (19 of 32 patients) and were related to the duration of stent implantation: 44 (72%) of 61 sections at ≤3 days (13 of 14 patients), 14 (78%) of 18 sections at 4 to 11 days (3 of 4 patients), 7 (24%) of 29 sections at 12 to 30 days (2 of 4 patients), and 0 of 34 sections at >30 days (0 of 11 patients ($P<0.0001$). The presence of platelet deposition around stent struts at ≤3 days was similar in Palmaz-Schatz stents (33 [80%] of 41 sections)

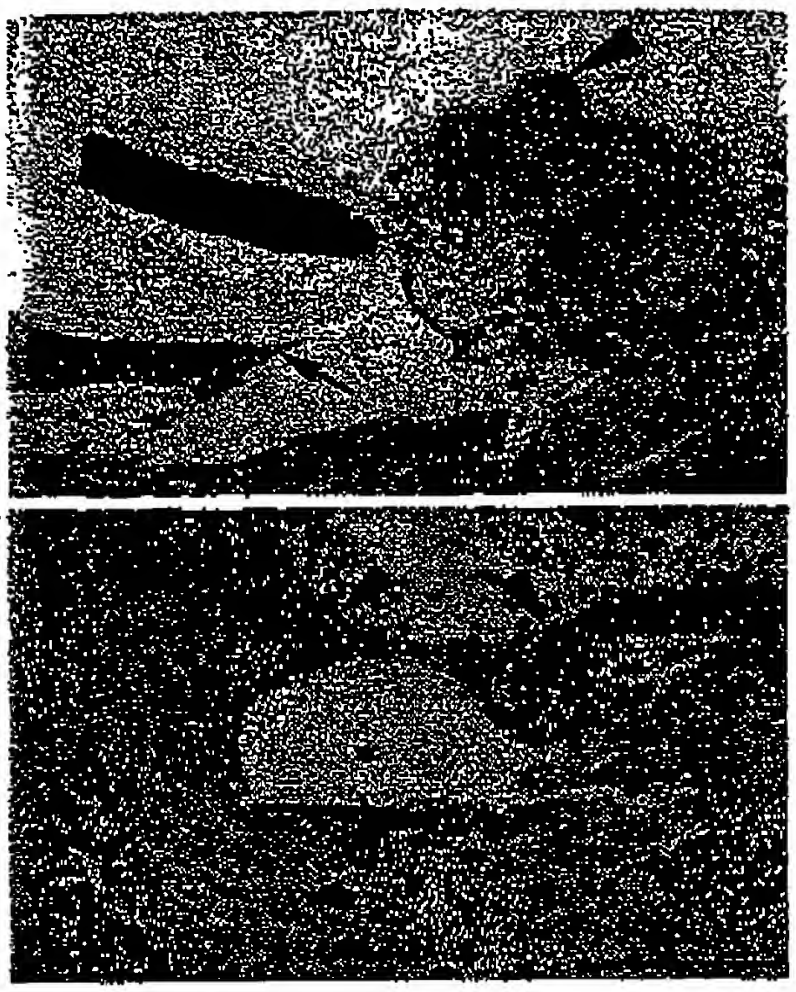

Figure 3. Platelet-rich thrombus (A, arrowhead) is associated with strut from Gianurco-Roubin II coronary artery stent implanted 1 day antemortem. Numerous acute inflammatory cells are present within the thrombus. Focal fibrous cap disruption is seen (arrow). A fibrin-rich thrombus (arrowheads) is focally present around a stent strut (*) 1 day after placement of a Palmaz-Schatz stent (B). Fibrous plaque (p) is present below the strut. (Hematoxylin-eosin; A, bar=0.16 mm; B, bar=0.12 mm.)

compared with Gianurco-Roubin stents (8 [62%] of 13 sections; P=NS). Fibrin-rich thrombi were also commonly seen around stent struts, especially early after stenting (Figure 3B). All 79 arterial sections from stents at ≤11 days (in 18 of 18 patients) had fibrin associated with stent struts; conversely, 12 (19%) of 63 sections and 7 of 14 patients at ≥12 days had stent fibrin (P<0.0001).

Acute inflammatory cells (neutrophils) associated with stent struts were present in 48 (79%) of 61 arterial sections and 12 of 14 patients in stents implanted for ≤3 days, 15 (83%) of 18 at 4 to 11 days (3 of 4 patients), 21 (72%) of 29 at 12 to 30 days (3 of 4 patients), and 0 of 34 at >30 days (P<0.0001 for all time points versus >30 days). Chronic inflammatory cells (lymphocytes and macrophages) around stent struts were also commonly seen at all time points: 50 (82%) of 61 sections at ≤3 days (11 of 14 patients), 12 (67%) of 18 sections at 4 to 11 days (3 of 4 patients), 28 (97%) of 29 sections at 12 to 30 days (4 of 4 patients), and 29 (85%) of 34 sections at >30 days (9 of 10 patients).

Inflammation associated with stents ≤3 days after implant in native coronary arteries was related to the underlying arterial wall morphology (Figures 4 and 5): 71% of struts in contact with fibrous plaque had ≤10 associated inflammatory

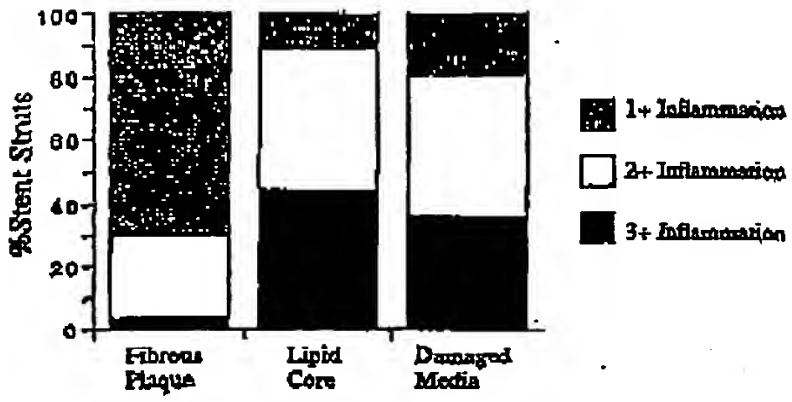

Figure 4. Inflammatory cell infiltrates associated with stent struts were assessed in coronary arteries containing stents of ≤3 days' duration. There were increased numbers of inflammatory cells associated with struts in contact with lipid core and damaged media compared with fibrous plaque (P<0.001). For grading scale, see Methods.

cells (1+ inflammation) compared with 11% of struts embedded in a lipid core and 19% of struts in contact with damaged media. In contrast, only 3% of struts in contact with fibrous plaque had 3+ inflammation (>20 associated inflammatory cells) compared with 44% of struts embedded in a lipid core and 36% of struts in contact with damaged media (P<0.001).

A neointima consisting of spindle-shaped mesenchymal cells (α-actin positive smooth muscle cells) within a proteoglycan matrix associated with stent struts was not present in any section in any of the 18 patients with ≤11 days implant duration; 45% of sections (2 of 4 patients) at 12 to 30 days (Figure 6) and 100% of sections (all 10 patients) at >30 days had spindle-shaped cells in a proteoglycan-rich matrix (P<0.0001). Multinucleated giant cells were present in only 3 (10%) of 29 sections at 12 to 30 days and were more frequently seen in older stents (10 [29%] of 34 sections at >30 days; Figure 7).

The findings in the 3 patients with stenting of saphenous vein grafts were similar to those in the 32 patients with stenting in native arteries. In a 3-day-old Palmaz-Schatz stent, the stent wires focally penetrated the thin fibrous cap and were embedded in the large necrotic core of the lipid-rich plaque, with the necrotic core prolapsing into the lumen (Figure 8). A well-defined neointima (smooth muscle cells in a proteoglycan-collagen matrix), focal plaque compression, and chronic inflammatory cells associated with stent struts were present in the 2 patients with chronic (120 and 270 days) Palmaz-Schatz stents in vein bypass grafts.

Arterial Injury and Coronary Stenting

There were a total of 1036 stent strut sites identified in the 137 sections of native coronary arteries, of which 643 (62%) of 1036 struts were in direct contact with atherosclerotic plaque. Of the remaining 393 struts (38%) in contact with the media, medial damage was present at 120 struts (30%) and medial compression without laceration of the internal elastic lamina (IEL) at 215 struts (55%); the media was unremarkable at 58 struts (15%). The mean arterial injury score (Schwartz scale[10]) for the arterial sections in which focal medial damage was present was 0.73±0.80. When medial damage was absent and stent struts were associated with a

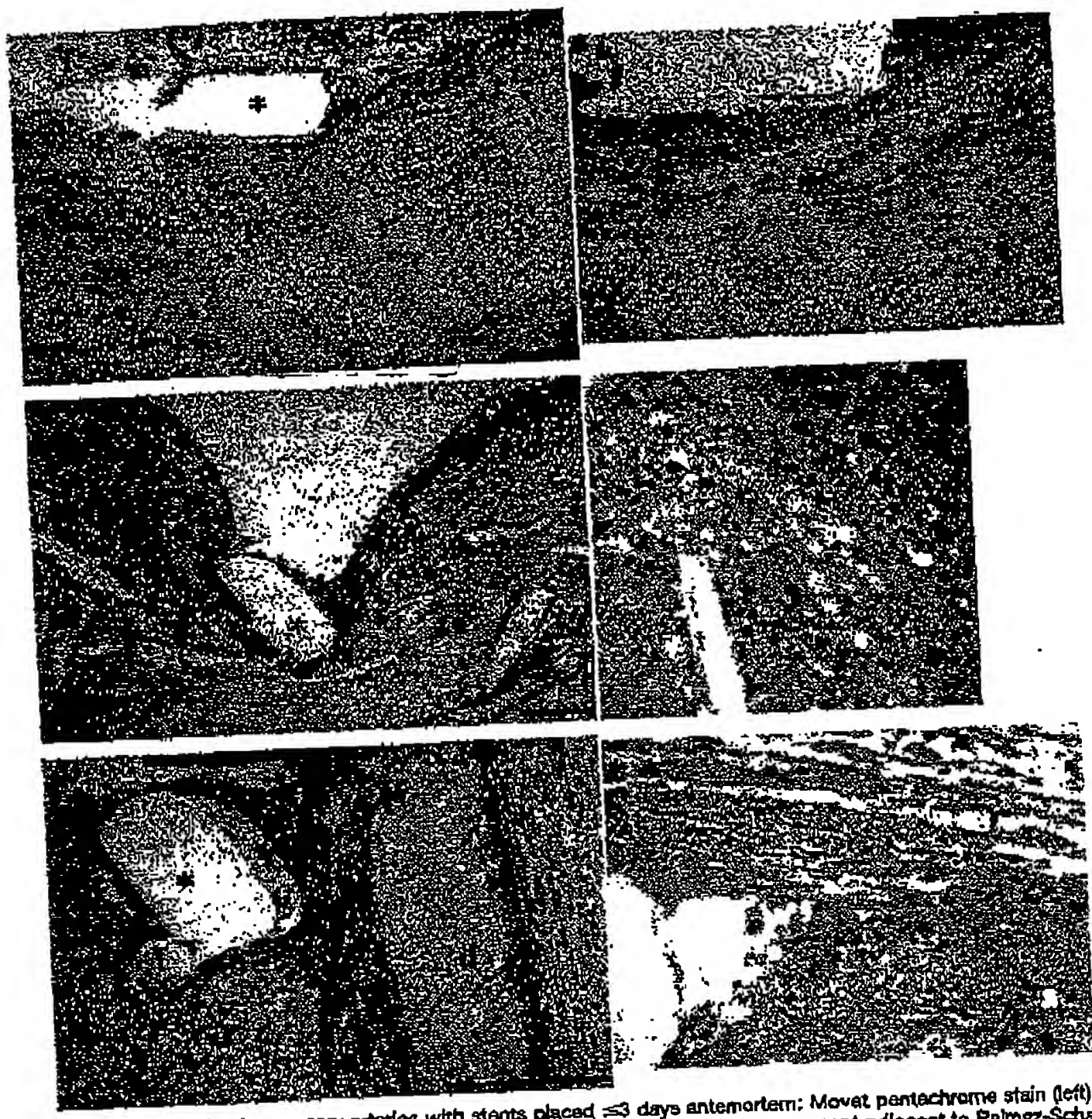

Figure 5. Arterial inflammation in coronary arteries with stents placed ≤3 days antemortem: Movat pentachrome stain (left) with higher-power hematoxylin-eosin staining (right) from same section. A, Few inflammatory cells are present adjacent to Palmaz-Schatz strut (*) in contact with fibrous plaque (p). B, Increased numbers of inflammatory cells are associated with Palmaz-Schatz strut (*) that penetrates into necrotic core (c). C, A Palmaz-Schatz strut (*) is in contact with damaged media (m) with dissection (d) and associated inflammatory cells. (A and B, bars=0.10 mm; C, bar=0.14 mm.)

normal or compressed media, the injury score was 0.11±0.21.

Neointimal Growth in Long-Term Stenting

In stents implanted for >30 days (mean, 175±105 days), neointimal thickness at stent strut sites was greater when medial damage (medial laceration or rupture) was present (0.69±0.29 mm) than when struts were in contact with plaque (0.33±0.26 mm; $P<0.0001$) or struts in contact with an intact media (0.29±0.23 mm, $P<0.0001$, Figure 9). Ultimate histological success was dependent on lumen area and neointimal growth within the stent (Table 2). The mean neointimal area and neointima area/stent area in successes were 2.2±1.1 and 0.39±0.12 mm², respectively, versus 3.9±1.9 and 0.68±0.15 mm² in failures, respectively ($P<0.006$ and $P<0.0001$). There were no differences between successes and failures with respect to areas of the external elastic lamina, IEL, plaque, or stent (Table 2). There was a significant linear correlation ($P<0.0001$, $R^2=0.54$) between increased neointimal growth and increased stent size relative to the proximal reference coronary artery lumen (Figure 10).

Chronic Stenting Versus PTCA: Neointimal Cellularity and Proteoglycans

The number of neointimal cells/mm² in native coronary arteries stented for >30 days was 3280±869, similar to that in PTCA arteries (3260±851 cells/mm²; Figure 11, A1-A2, B1-B2) matched for time since treatment (195±131 days for stents and 180±137 days for PTCA). The neointimal area

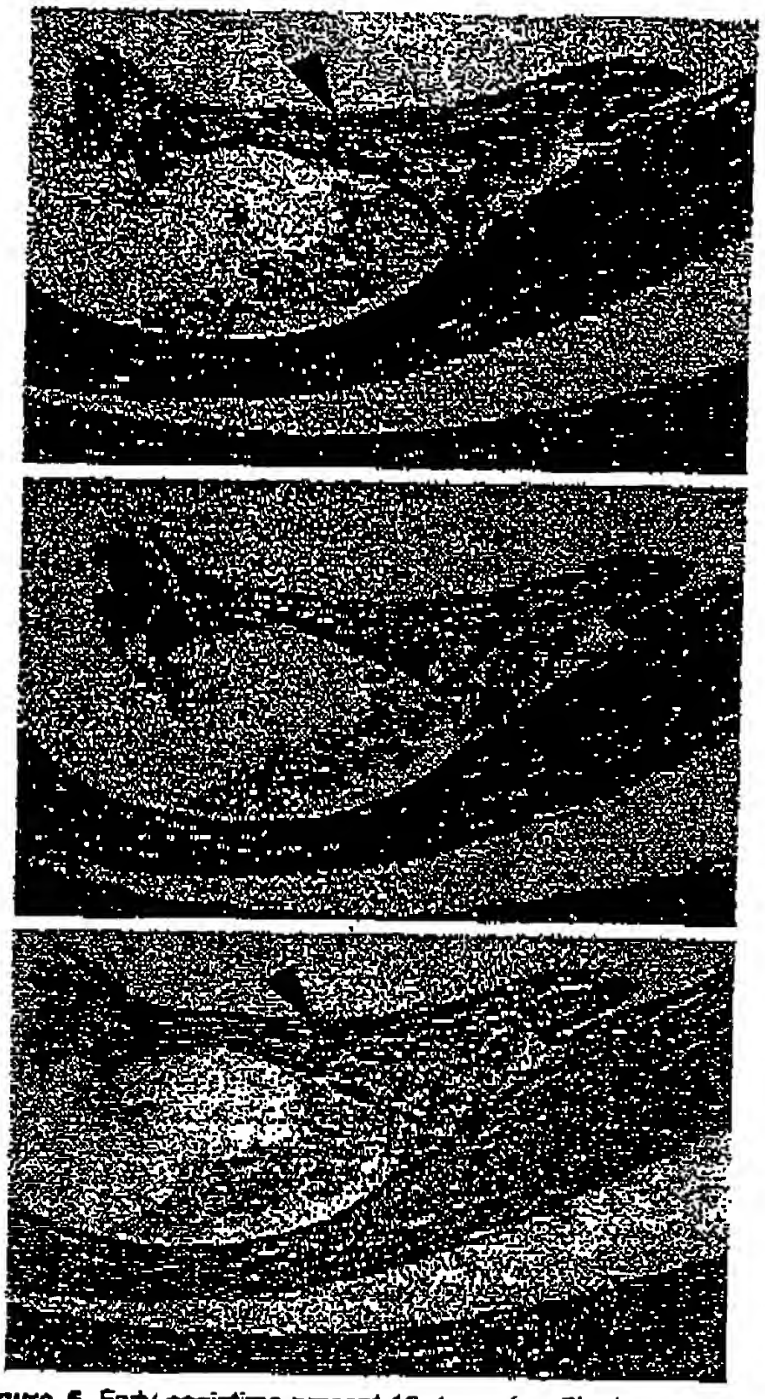

Figure 6. Early neointima present 12 days after Gianturco-Roubin coronary artery stent placement. A, Intimal cells within extracellular matrix (arrowhead) are seen above the stent strut. B, KP-1 immunostaining identifies macrophages adjacent to the strut at base of neointima (arrow). C, Actin staining shows smooth muscle cells close to luminal surface of neointima (arrowhead), within the plaque close to the media, and within the media (m). (A: Movat pentachrome, bar=0.16 mm; B: KP-1 immunostain; C: smooth muscle actin immunostain.)

was greater in the stented segments than in PTCA arteries (3.1±1.6 versus 1.9±1.2 mm², respectively; $P<0.05$). However, IEL area was larger (11.6±2.1 mm²) with stent placement than with PTCA (7.9±2.1 mm², $P=0.0001$), so that the neointima corrected for artery size (neointima/IEL) was similar in stents and PTCA (0.26±0.16 versus 0.26±0.10, respectively; P=NS). The mean neointimal thickness in the stented arteries (0.39±0.26 mm) was smaller than in PTCA vessels (0.51±0.24 mm), but this difference did not reach statistical significance.

Alcian blue staining of stented and matched PTCA arteries demonstrated similar patterns of neointimal proteoglycan deposition. Alcian blue staining showed strong blue staining of the neointima in stented and PTCA arteries (Figure 11, A3 and B3). After testicular hyalidase digestion, there was similar light staining for heparan and dermatan sulfate in stented and PTCA arteries (Figure 11, A4 and B4). These data identify chondroitin

Figure 7. Multinucleated giant cell (arrowhead) and numerous chronic inflammatory cells (ic) associated with Palmaz-Schatz stent strut (*) placed 70 days antemortem in the left anterior descending coronary artery. (Hematoxylin-eosin, bar=0.10 mm.)

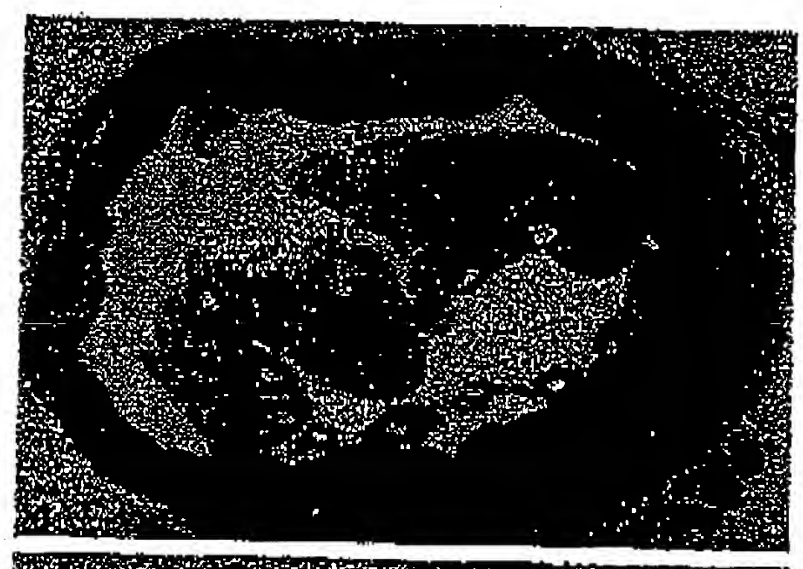

Figure 8. Palmaz-Schatz stent placed 3 days antemortem in a saphenous vein graft containing a large necrotic core (nc, low power in A). In B (high power), there is focal extrusion of necrotic core contents (outlined by arrowheads) into the lumen secondary to penetration of stent struts into the lipid core. The protruding necrotic core is covered by a layer of thrombus (t). (Movat pentachrome; bar=0.14 mm.)

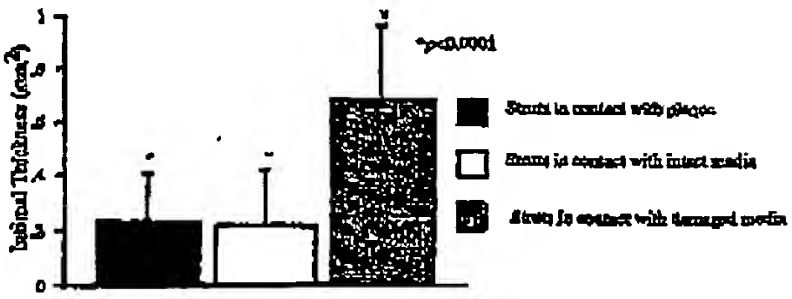

Figure 9. In stents implanted for >30 days, neointimal thickness was increased at stent strut sites when medial laceration or rupture was present compared with struts in contact with plaque or with an intact media.

sulfate and hyaluronic acid as the predominant neointimal proteoglycans in PTCA and stented arteries.

Discussion

The present study demonstrates the time course of histological vascular responses to coronary stenting in humans. Early after stenting (≤11 days), fibrin, platelets, and acute inflammatory cells were nearly always present in association with stent struts. The stent–arterial wall interface influenced the severity of associated inflammation; increased numbers of inflammatory cells were seen when the stent strut was adjacent to injured media or lipid core rather than fibrous plaque. Chronic inflammation was also commonly observed adjacent to stent struts at all time points, especially ≥12 days after stenting. Plaque was compressed by stent struts (seen in 91% of vessel sections) in the present study. However, the concept that stents provide a boundary that excludes the underlying plaque from the lumen was not supported by the present study; penetration of the stent struts into a lipid core was common (26% of arterial sections with a lipid core had stent struts embedded in the core). A neointima containing smooth muscle cells was recognized beginning ~2 weeks after stenting.

In longer-term stents (>30 days after implant), histological success or failure was determined by neointimal growth within the stent and was not influenced by artery or stent size. Neointimal thickness was increased when medial damage was present compared with struts in contact with atherosclerotic plaque or an intact media. Furthermore, increased intrastent neointimal growth was present in histological failures, and increased neointimal area correlated with increased stent size relative to the proximal reference artery lumen. Therefore, stent oversizing relative to the reference lumen appears to be an undesirable goal in deployment. Intravascular ultrasound may be particularly useful in determining proximal reference lumen area. A stenting strategy in which stents are expanded to a point at which no gradient exists from the proximal reference to the stent may be beneficial. The present study is the first to compare whole arterial sections and to show neointimal cell density and type of proteoglycan deposition in coronary stents similar to those in matched PTCA coronary vessels. In these arteries, the neointimal area was greater in stented arteries than in arteries with PTCA, but this difference was accounted for by the larger vessel size in the stent group.

TABLE 2. Morphometric Data from Histological Sections of Native Coronary Arteries Containing Stents >30 Days' Duration

	Histological Success (n=16)	Histological Failure (n=14)	P
EEL area, mm²	10.9±4.0	10.9±2.3	0.98
IEL area, mm²	9.7±3.5	9.9±2.2	0.89
Stent area, mm²	5.9±2.7	5.5±1.7	0.60
Plaque area, mm²	3.8±1.3	4.4±1.8	0.31
Neointima area, mm²	2.2±1.1	3.9±1.9	<0.006
Neointima area/stent area	0.39±0.12	0.68±0.15	<0.0001
Lumen area, mm²	3.7±1.9	1.6±0.6	<0.0006

A long-term histological success was defined as a percent area stenosis ≤75%. A long-term histological failure was defined as a percent area stenosis >75%.

EEL indicates external elastic lamina. Values are mean±SD.

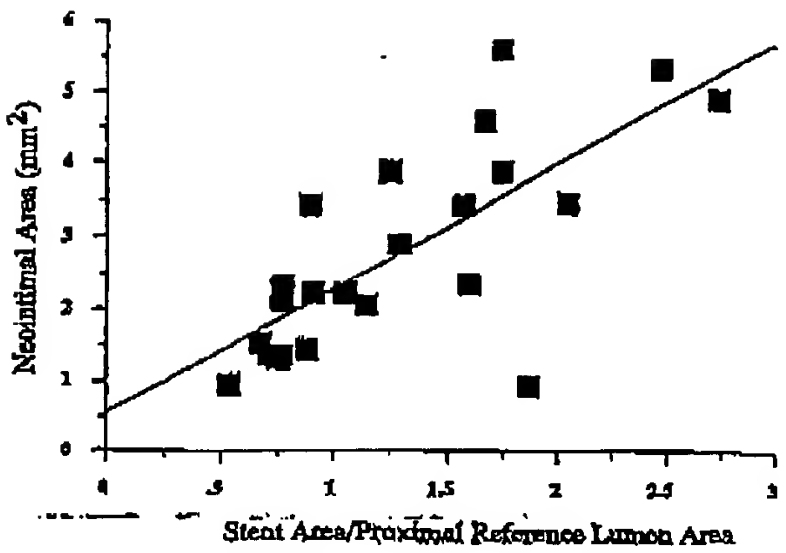

Figure 10. Linear regression comparing ratio of stent area to lumen area of proximal reference artery (*x* axis) to that of neointimal area (*y* axis). Increased neointimal growth was associated with increased stent size relative to proximal reference lumen (R^2=0.54, P<0.0001).

Previous Pathological Studies of Stenting in Humans

Few pathological observations of coronary stenting in humans have been reported. Anderson et al[6] reported pathological findings in 4 cases of Gianturco-Roubin stenting in coronary vessels: 2 native coronary arteries and 2 coronary bypass vein grafts. At 21 days, stent endothelialization was present, and a thin neointima containing smooth muscle cells was seen.[6] In vein grafts at 19 weeks and 6 months, a smooth muscle cell–rich neointima and occasional chronic inflammatory cells were seen.[6] In a study of 11 human coronary stents, 4 of which were placed for restenosis after PTCA, Komatsu et al[9] showed actin-positive intimal smooth muscle cells 30 days after stenting. Van Beusekom et al[7] studied saphenous vein coronary bypass grafts with Wallstents (21 stents in 10 patients). At 3 days, leukocytes, platelets, and fibrin were evident, and at 3 months, there was complete endothelial stent coverage and a smooth muscle cell–rich neointima. At 6 to 10

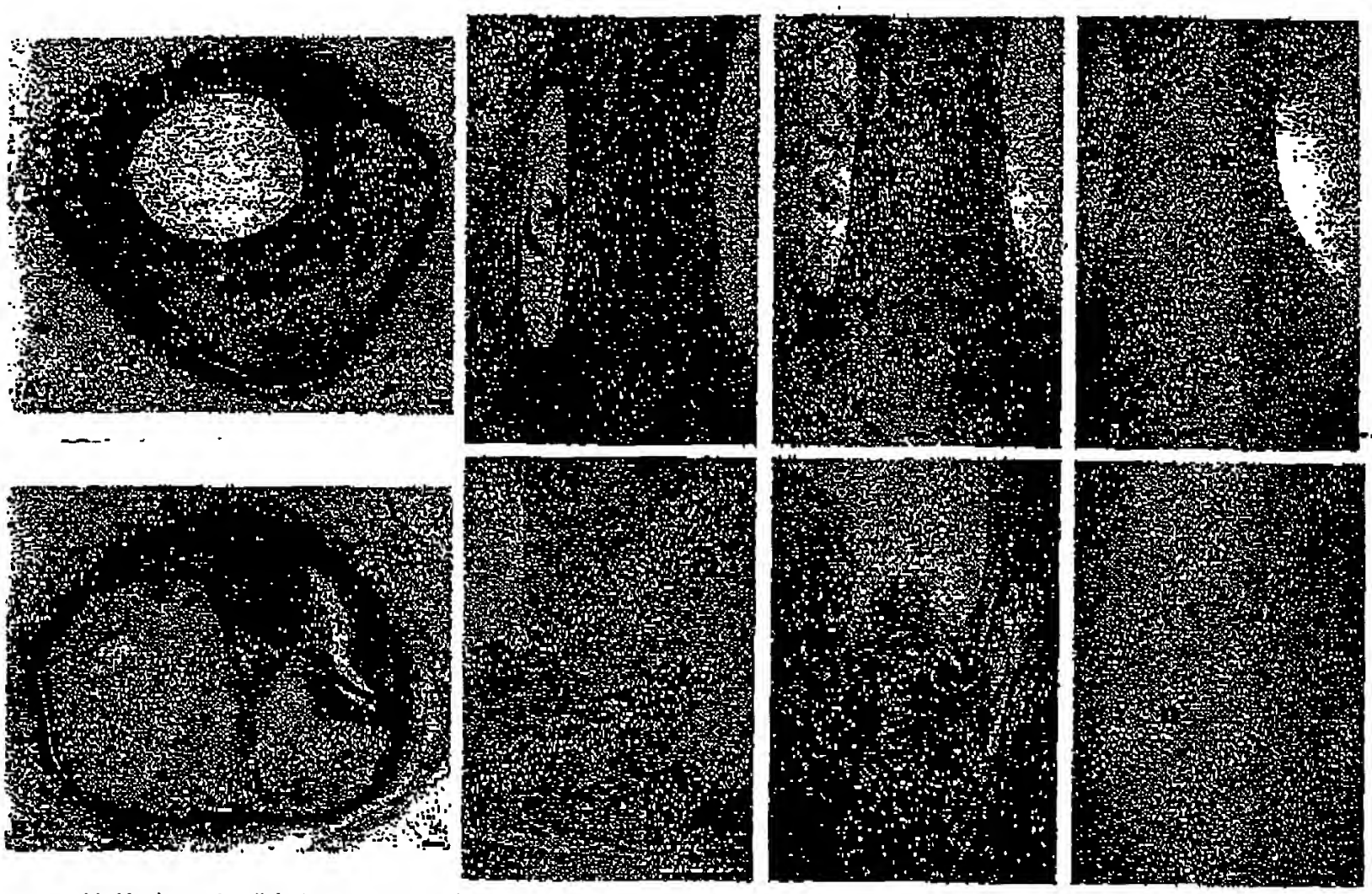

Figure 11. Neointimal cellularity and proteoglycans in chronic coronary stents compared with balloon angioplasty (PTCA). A1, Low-power micrograph of left circumflex coronary artery containing Gianturco-Roubin stent placed 10 months antemortem. Neointima is outlined by arrowheads, and stent strut is identified (*). Neointima is relatively thicker over stent strut compared with remainder of arterial segment. Bar=0.20 mm. A2, α-Actin staining of neointima (n) identifying smooth muscle cells bar=0.12 mm. A3, Strong Alcian blue stain of neointima (n) showing presence of proteoglycans; bar=0.12 mm. A4, Faint Alcian blue staining after testicular hyalidase digestion, identifying minimal heparan sulfate and dermatan sulfate glycosaminoglycans in neointima (n). Strong Alcian blue staining before testicular hyalidase digestion indicates that neointimal proteoglycans consist predominantly of chondroitin sulfate and hyaluronic acid. Bar=0.12 mm. B1, Low-power micrograph of left anterior descending coronary artery treated with PTCA 13 months antemortem. Neointima is outlined by arrowheads, and residual lumen (L) is indicated. Bar=0.16 mm. B2, α-Actin staining of neointima (n), identifying smooth muscle cells. Cell density is similar to stented artery (A2). Bar=0.20 mm. B3, Alcian blue stain of neointima (n) showing strong staining for proteoglycans, similar in intensity to stented artery (A3). Bar=0.08 mm. B_4, Faint Alcian blue staining after testicular hyalidase digestion, identifying minimal heparan sulfate and dermatan sulfate glycosaminoglycans in neointima (n), similar in intensity to stented artery (A4). Chondroitin sulfate and hyaluronic acid are the major constituents of the neointimal proteoglycans after PTCA. Bar=0.08 mm. (A1 and B1, Movat pentachrome; A2 and B2, smooth muscle actin immunostain; A3 and B3, Alcian blue; and A4 and B4, Alcian blue with 3 hours' hyaldase digestion.)

months, atherosclerotic plaque, foam cells, and cholesterol crystals were observed; it was suggested that stent-induced atheroma formation may occur.[7] In the present study, the neointima was composed of smooth muscle cells in a proteoglycan-rich matrix. The presence of atherosclerotic plaque within the stent is likely due to penetration of struts into the necrotic core and prolapse of plaque between stent wires rather than stent-induced accelerated atherosclerosis.

Comparison to Stenting in Experimental Animal Models

In the porcine restenosis model, thrombus adjacent to stent struts composed of fibrin and trapped erythrocytes with acute inflammatory cells is seen at 24 hours.[11] At 7 days, there is organization of the thrombus associated with macrophages; however, neutrophils are still observed.[11] From 14 to 28 days after stenting, smooth muscle cells are the predominant cell type, with occasional chronic inflammatory cells present.[11] These data in the pig model regarding inflammation and thrombus closely reflect the findings observed in human coronary stenting early after implantation (with a relatively longer duration of healing in humans).

The type of vascular injury in stented normal arteries in experimental animals differs considerably from that in human atherosclerotic arteries. In normal pig arteries, for example, stent oversizing to produce a proliferative neointimal lesion results in direct medial injury (compression or laceration) by stent struts. In contrast, in humans, we observed that 62% of stent struts were in direct contact with atherosclerotic plaque, not media; medial compression by stent struts or medial damage associated with struts was present at 32% of struts.

Arterial Inflammation and Injury: Clinical Implications

Experimental studies suggest important relationships among inflammation, vascular injury, and neointimal growth. In stented, nonatherosclerotic, balloon-injured rabbit iliac arteries, peak monocyte adherence was observed 3 days after stenting, with maximal proliferation seen at 7 days.[12] There was a linear correlation (R^2=0.82 to 0.92) between monocyte adherence and neointima at 14 days.[12] Furthermore, increased vascular injury correlated with increased neointimal growth, inflammation, and thrombus formation.[13] In the porcine double-artery injury model, neointimal thickness was smaller at strut sites adjacent to an intact IEL and media than at areas of medial loss.[14] The observations from experimental work showing correlations among arterial injury, inflammation, and neointima and data from the present study demonstrating increased inflammation associated with stent struts in the vicinity of damaged media and increased neointimal thickness at struts associated with medial damage suggest that avoidance of severe arterial injury during catheter-based interventions with stents may have a beneficial effect on late neointimal growth. Data from the present study showing the positive association of neointimal growth and increased stent sizing relative to the proximal reference lumen (a reflection of probable increased arterial injury) are supportive of stent-deployment techniques that can reduce arterial injury. Novel devices that do not require very high balloon inflations to accomplish close apposition of the stent to the arterial wall (eg, self-expanding stents) are currently under clinical trial.

Limitations

The findings in the present study are derived from descriptive pathology. Because most of the tissues analyzed were obtained at autopsy, the results presented may not be representative of persons who receive stents and survive. However, the present study is the first to report histological findings from a large series of stents placed in native human coronary arteries, and a majority of segments with stents in place for >30 days demonstrated histological success.

Conclusions

Morphology after coronary stent placement demonstrates the following sequence of events: thrombus formation and acute inflammation early after deployment, with subsequent neointimal growth. Increased inflammation early after stenting is associated with medial injury and lipid core penetration by stent struts. Medial damage and stent oversizing relative to the reference arterial lumen are associated with increased neointimal growth.

References

1. Schomig A, Kastrati A, Dietz R, Rauch B, Neumann F-J, Kates RH, Busch U. Emergency coronary stenting for dissection during percutaneous transluminal coronary angioplasty: angiographic follow-up after stenting and after repeat angioplasty of the stented segment. *J Am Coll Cardiol*. 1994; 23:1053–1060.
2. Serruys PW, de Jaegere P, Kiemeneij F, Macaya C, Rutsch W, Heyndrickx G, Emanuelsson H, Marco J, Legrand V, Materne P. A comparison of balloon-expandable stent implantation with balloon angioplasty in patients with coronary artery disease. *N Engl J Med*. 1994;331:489–495.
3. Fischman DL, Leon MB, Baim DS, Schatz RA, Savage MP, Penn I, Detre K, Veltri L, Ricci D, Nobuyoshi M. A randomized comparison of coronary stent placement and balloon angioplasty in the treatment of coronary artery disease. *N Engl J Med*. 1994;331:496–501.
4. Thomas CN, Weintraub WS, Shep Y, Ghazzal ZM, Douglas JS, King SB III, Scott NA. "Bailout" coronary stenting in patients with a recent myocardial infarction. *Am J Cardiol*. 1996;77:653–655.
5. Klugherz BD, DeAngelo DL, Kim BK, Herman RC, Hirshfeld JW, Kolansky DM. Three-year clinical follow-up after Palmaz-Schatz stenting. *J Am Coll Cardiol*. 1996;27:1185–1191.
6. Sawada Y, Nosaka H, Kimura T, Nobuyoshi M. Initial and six month outcome of Palmaz-Schatz stent implantation: STRESS/Benestent equivalent vs non-equivalent lesions. *J Am Coll Cardiol*. 1996;27(suppl A):252A. Abstract.
7. Van Beusekom HMM, Van der Giessen WJ, Van Suylen RJ, Bos E, Bosman FT, Serruys PW. Histology after stenting of human saphenous vein bypass grafts: observations from surgically excised grafts 3 to 320 days after stent implantation. *J Am Coll Cardiol*. 1993;21:45–54.
8. Anderson PG, Bajaj RK, Baxley WA, Roubin GS. Vascular pathology of balloon-expandable flexible coil stents in humans. *J Am Coll Cardiol*. 1992;19:272–381.
9. Komatsu R, Ueda M, Naruko T, Kolirsa A, Becker AE. Neointimal tissue response at sites of coronary stenting in humans: macroscopic, histological, and immunohistochemical analysis. *Circulation*. 1998;98:224–233.
10. Schwartz RS, Huber KC, Murphy JG, Edwards WD, Camrud AR, Vlietstra RE, Holmes DR. Restenosis and the proportional neointimal response to coronary artery injury: results in a porcine model. *J Am Coll Cardiol*. 1992;19:267–274.
11. Carter AJ, Laird JR, Farb A, Kufs W, Wortham DC, Virmani R. Morphologic characteristics of lesion formation and time course of smooth muscle cell proliferation in a porcine proliferative restenosis model. *J Am Coll Cardiol*. 1994;24:1398–1405.
12. Rogers C, Welt FGP, Karnovsky MJ, Edelman ER. Monocyte recruitment and neointimal hyperplasia in rabbits: coupled inhibitory effects of heparin. *Arterioscler Thromb Vasc Biol*. 1996;16:1312–1318.
13. Rodes C, Edelman ER. Endovascular stent design dictates experimental restenosis and thrombosis. *Circulation*. 1995;91:2995–3001.
14. Carter AJ, Laird JR, Kufs WM, Bailey L, Hoopes TG, Reeves T, Farb A, Virmani R. Coronary stenting with a novel stainless steel balloon-expandable stent: determinants of neointimal formation and changes in arterial geometry after placement in an atherosclerotic model. *J Am Coll Cardiol*. 1996;27:1270–1277.